ELSEVIER

Mass transfer, kinetics and equilibrium studies for the biosorption of methylene blue using *Paspalum notatum*

K. Vasanth Kumar [a,*], K. Porkodi [b]

[a] *Department of Chemical Engineering, AC College of Technology, Anna University, Chennai 600025, TN, India*
[b] *CIQ-UP, Department of Chemistry, Faculty of Science, University of Porto, Rua do Campo Alegre 687, 4169-007 Porto, Portugal*

Abstract

Batch experiments were carried out for the sorption of methylene blue onto *Paspalum notatum*. The operating variables studied were initial dye concentration, initial solution pH, adsorbent dosage and contact time. Experimental equilibrium data were fitted to Freundlich, Langmuir and Redlich–Peterson isotherms by non-linear regression method. Six error functions was used to determine the optimum isotherm by non-linear regression method. The present study shows r^2 as the best error function to determine the parameters involved in both two- and three-parameter isotherms. Langmuir isotherm was found to be the optimum isotherm for methylene blue onto *P. notatum*. The monolayer methylene blue sorption capacity of *P. notatum* was found to be 31 mg/g. The kinetics of methylene blue onto *P. notatum* was found to follow a pseudo second order kinetics. A Boyd plot confirms the external mass transfer as the rate-limiting step in the dye sorption process. The influence of initial dye concentration on the dye sorption process was represented in the form of dimensionless mass transfer numbers ($Sh/Sc^{0.33}$) and was found to vary as $C_0^{-5\times10^{-6}}$.
© 2006 Elsevier B.V. All rights reserved.

Keywords: Biosorption; Methylene blue; *Paspalum notatum*; Kinetics; Equilibrium; Mechanism; Isotherm

1. Introduction

Most of the synthetic dyes are extensively used in several fields such as in textile industries, leather tanning, paper production, food technology, agricultural research, light harvesting arrays, petrochemical cells and in hair colorings [1]. Textile industries are responsible for the discharge of large quantities of dyes into natural waterways due to the inefficiencies in dyeing techniques [2]. Color is a visible pollutant and presence of even very minute amount of coloring substance makes it undesirable due to its appearance. The removal of color from dye bearing effluents is one of the major problem due to the difficulty in treating such wastewaters by conventional treatment methods. Dyes may be problematic and may produce into toxic amines if they are broken down anaerobically in the sediment due to incomplete degradation by bacteria [3]. Chemical treatment process such as photocatalytic degradation process may pro-

duce concentrated sludge such as Fentons reagent. Membrane filtrations are incapable of treating large volumes. Activated carbon adsorption processes are currently proved to be a highly effective process for the removal of dye from wastewaters. However this process is found to be expensive due to the high cost of activated carbon. Thus there is a continuous search for an equally or nearly equal and efficient but cheaper sorbent. The use of biomaterials as sorbents for the treatment of wastewaters will provide as a potential alternate to the conventional treatment methods [4,5]. The process of uptake of solute using biomaterials (microbial cells), whether dead or alive, is known as biosorption [4]. In the present investigation, the biomass of *Paspalum notatum* (garden grass) was used as biosorbent and its capacity to remove methylene blue a basic (cationic) dye was evaluated. A survey of literature showed that no work has been done so far on dye removal process using *P. notatum* as biosorbent for the removal of dye stuffs from their aqueous solutions. Methylene blue has wider applications, which include coloring paper, coloring leather products, dyeing cottons, wools, temporary hair colorant, coating for paper stock etc. Though methylene blue is not strongly hazardous, it can cause some harmful effects. Acute exposure to methylene blue will found
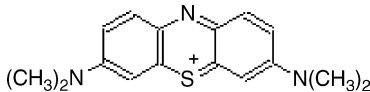
Nomenclature

A	Redlich–Peterson isotherm constant
ARE	the average relative error
B	Redlich–Peterson isotherm constant (in Eq. (5))
B	Boyd's constant (in Eq. (13))
C	concentration at any time t (mg/L)
C_e	equilibrium concentration (mg/L)
C_0	initial dye concentration (mg/L)
d_p	particle diameter (cm)
D_{AB}	diffusivity of methylene blue in solvent (cm^2/s)
D_i	effective diffusivity (cm^2/s)
EABS	the sum of the absolute errors
ERRSQ	the sum of the squares of the error
F	fraction of available adsorption sites at any time t
g	Redlich–Peterson constant
HYBRID	the hybrid fractional error function
k_1	pseudo first order rate constant (min^{-1})
k_2	pseudo second order rate constant (g/(mg min))
k_i	intraparticle diffusion constant (mg/(g min$^{0.5}$))
K_a	Langmuir isotherm constant (L/mg)
K_F	Freundlich constant (mg/g)(L/g)$^{1/n}$
K_s	external mass transfer coefficient (cm/s)
M	Adsorbent mass (g)
M_B	molecular weight of solute
MPSD	Marquardt's percent standard deviation
n	Freundlich exponent
n	number of experimental measurements (in Table 2)
p	number of parameters in isotherm
q	amount of dye adsorbed at any time t (mg/g)
q_e	amount of dye adsorbed at equilibrium (mg/g)
q_m	monolayer sorption capacity (mg/g)
r	particle radius
$r_{\text{Rapid phase}}$	rate of reaction in the rapid phase (mg/(g min))
$r_{\text{Slower phase}}$	rate of reaction in the slower phase (mg/(g min))
r^2	coefficient of determination
S	surface area of adsorbent per unit volume of particle free slurry (cm^{-1})
t	contact time (min)
T	temperature (K)
V	volume of dye solution (L)
V_A	molal volume of solute

Greek symbols

ε_p	bed porosity
μ	dynamic viscosity of solute
ρ	bulk density (g/cm^3)
υ	kinematic viscosity (cm^2/s)
Φ	association factor of solvent

cause increased heart rate, vomiting, shock, Heinz body formation, cyanosis, jaundice, quadripelgia and tissue necrosis in humans [6]. In the present study, methylene blue is selected as a model compound in order to evaluate the capacity of *P. notatum*

Table 1
Information of dye used

C.I. number	52015
C.I. name	Basic blue 9
Empirical formula	$C_{16}H_{18}N_3SCl$
Formula weight	319.9
Absorption maximum	665 nm
Structure	

for the removal of dye (methylene blue) from its aqueous solutions.

2. Materials and methods

2.1. Biosorbent

The dried *P. notatum* was collected from the Anna University main campus garden, Chennai, TN. The collected materials were further dried under sunlight for 48 h. The dried materials were then grinded using a domestic Sumeet mixer and the particle size in the range of 60–80 mesh (BSS) were used as biosorbents for the present study.

2.2. Sorbate

The dye used in all the experiments was methylene blue, a basic (cationic) dye. The dye methylene blue was obtained from Ranbaxy Chemicals, Mumbai. Synthetic stock dye solutions were prepared by dissolving 1 g of methylene blue in 1 L of double distilled water. All working solutions were prepared from the stock solutions by further dilution. The NaOH pellets and HCl solution used for optimizing pH are obtained from Qualigens fine chemicals, Mumbai. The structure and other information of dyes are shown in Table 1.

2.3. Process

2.3.1. Effect of pH

The effect of pH on the amount of color removal was analyzed over the pH range from 3 to 8. The pH was adjusted using NaOH and HCl solutions. In this study 30 mL of dye solution of 100 mg/L of dye/L was agitated with 0.04 g of *P. notatum* for 6 h, which is more than sufficient to reach equilibrium. The equilibrium time was determined based on several trial experiments carried out for different initial dye concentration. The trial experiments showed that equilibrium time was varied between 4 and 5 h. Thus in the present study 6 h of contact time was provided in order to assure that equilibrium was achieved. The samples were then centrifuged and the left out concentration in the supernatant solution were analyzed using UV Spectrophotometer (Deep Vision 301 E) by monitoring the absorbance changes at a wavelength of maximum absorbance (665 nm). For all the experiments, except the adsorption kinetics, the contact was made using water bath shakers at 303 K and at a constant agitation speed of 95 rpm.

2.3.2. Effect of biosorbent mass

The effect of biosorbent mass on the amount of color adsorbed was obtained by agitating 30 mL of dye solution of initial dye concentration of 100 mg/L with weighed amount of *P. notatum* (ranging from 0.01, 0.02, 0.03, 0.04, 0.05, 0.06, 0.07 and 0.08 g) till equilibrium is reached.

2.3.3. Biosorption equilibrium

Equilibrium experiments were performed by contacting 0.04 g of *P. notatum* particles with 30 mL of dye solution of different initial dye concentration ranging from 30 mg/L to 100 mg/L.

2.3.4. Biosorption kinetics

Sorption kinetics experiments were carried out at different initial dye concentrations using laboratory over head stirrers. Kinetic experiments were carried out by agitating 2 L of dye solution of known initial concentration with 2.67 g of *P. notatum* at a constant agitation speed of 800 rpm. Definite volume of 2.5 mL of samples were pipetted out at time intervals of 2, 4, 6, 8, 10, 20, 30 and 60 min. The collected samples were then centrifuged and the concentration in the supernatant solution were determined using UV spectrophotometer.

2.3.5. Dye uptake

The amount of dye sorbed onto unit weight of biosorbent and % color removal were calculated using the following equations, respectively:

$$q = \frac{(C_0 - C)V}{M} \tag{1}$$

$$\%\text{removal} = \frac{C_0 - C}{C_0} \times 100 \tag{2}$$

where C_0 is the initial dye concentration (mg/L), C the concentration of dye at any time t, V the volume of solution (L) and M is the mass of biosorbent (g).

3. Results and discussions

3.1. Effect of pH

Fig. 1 shows the effect of initial solution pH on the amount of dye adsorbed (mg/g) at equilibrium conditions. From Fig. 1, it was observed that the amount of dye adsorbed exponentially gets increased with increase in pH. The amount of dye adsorbed gets increased from 21.69 mg/g to 26.10 mg/g for an increase in pH from 3 to 8. The initial solution pH influences both the binding sites in the biosorbent surface and also the solution chemistry. The *P. notatum* is a complex material containing lignin and cellulose. The influence of the solution pH on the dye uptake can be explained on the basis of the zero point charger or isoelectric point of the biosorbent. The ionic state of ligands such carboxyl, phosphate and amino groups in the lignin based materials would promote the reaction with dye ions [7]. The zero point charge pH$_{zpc}$ of the biosorbent was determined using powder addition method. 0.5 g of biosorbent was added to round bottom flask
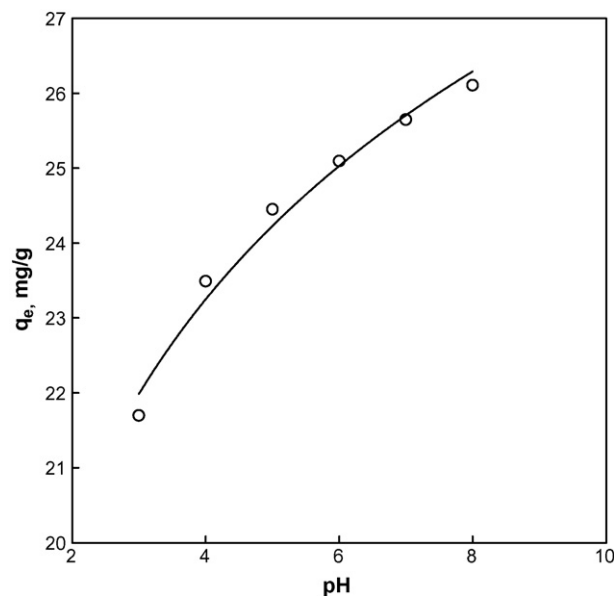

Fig. 1. Effect of initial pH for the removal of methylene blue by *P. notatum* (C_0, 100 mg/L; V, 0.03 L; M, 0.04 g).

containing 50 mL of NaCl solution. Two sets of experiments were carried out with 0.1 M NaCl and 0.01 M NaCl solution. Several batches were carried out for various initial solution pH, called pH$_0$. The pH was adjusted using 0.1 M HCl and NaOH solution. The electrolyte solution with the biosorbent was equilibriated for 24 h. After equilibriation, the final pH, pH$_{final}$ was recorded. The point at which the difference between the initial and final pH equivalent to zero was recorded as zero point of charge of the biomaterial. The zero point charge of *P. notatum* was found to be 4.6. At the pH > pH$_{zpc}$, the surface of the biosorbent gets negatively charged thereby supporting the more dye uptake due to electrostatic force of attraction. At lower pH (pH < pH$_{zpc}$), the H$^+$ ions compete effectively with dye cations causing a decrease in q_e. This can be observed from the higher and lower sorption capacity at higher and lower pH, respectively.

3.2. Effect of adsorbent mass

Fig. 2(a) shows the plot of equilibrium uptake capacity, q_e (mg/g) and % color removal against biomass concentration (g). From Fig. 2(a), it was observed that the amount of dye adsorbed onto unit weight of biosorbent gets decreased with increasing biomass concentration. The dye uptake decreased from 33.6 mg/g to 18.34 mg/g for an increase in biomass concentration from 0.01 g to 0.08 g. Whereas the % color removal increases from 11.2% to 48.9% for an increase in adsorbent dosage from 0.01 g to 0.08 g. The increase in % color removal is due to the increase in the vacant adsorption sites with increasing biomass thus favoring more dye uptake (in %). The decrease in q_e value may be due to the splitting effect of flux (concentration gradient) between sorbate and sorbent with increasing biomass concentration causing a decrease in amount of dye adsorbed onto unit weight of biomass produces a lower solute concentration in the solution than when biomass concentration is lower.
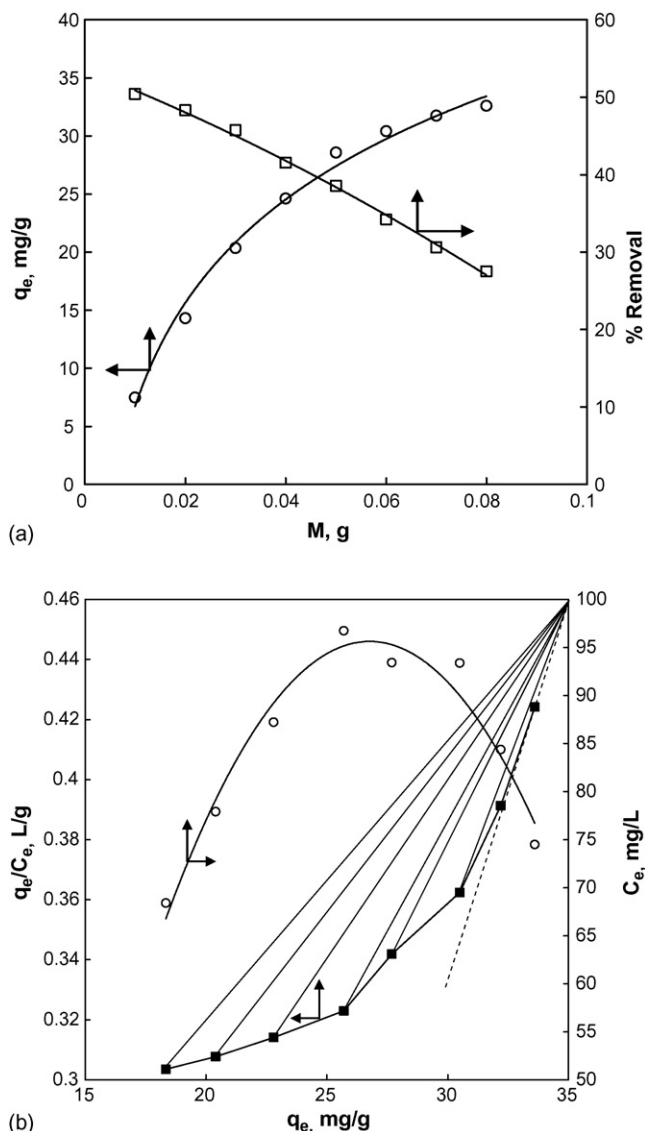
Fig. 2. (a) Effect of *P. notatum* mass on the uptake of methylene blue (C_0, 100 mg/L; pH 8) and (b) plot of q_e/C_e vs. q_e for different operating ($-V/X$ ratio) lines (C_0, 100 mg/L; pH 8).

This can be explained on the basis of initial concentration gradient between the solid adsorbent and the bulk liquid. For a fixed volume of dye solution and for a fixed initial dye concentration, the initial concentration gradient between the adsorbent and the dye solution gets decreased with increasing initial dye concentration. It is likely that the amount of dye adsorbed onto unit weight of adsorbent gets increased with the driving force, i.e. the initial concentration gradient. However in this case for a fixed volume of dye solution and initial dye concentration, the initial concentration gradient between the adsorption vacant sites of the solid adsorbent and the concentration of dye solution gets decreased with increasing adsorbent mass leading to decrease in q_e value. In the present study, from Fig. 2(a), it can be observed that for all the sorbate mass studied, the concentration in dye solution was in excess to that of the maximum vacant sties available at the surface of the adsorbent. However the q_e value still found to decrease with increasing sorbate mass. This effect

may be attributed due to the reduction in overall surface area of the biosorbent probably because of aggregation during the sorption [6,7]. From Fig. 2(a), it is observed that the amount of q_e was found to decrease exponentially with increasing biomass concentration. This effect can be explained on the basis of solute distribution between the biosorbent and bulk dye solution. The solute distribution between the sorbent and the bulk solution can be visualized from the plot of q_e/C_e versus q_e as shown in Fig. 2(b). The slope of Fig. 2(b) will give the left out solution concentration in the bulk solution. From Fig. 2(b), it was observed that there exist a parabolic relation between q_e/C_e versus q_e. The concentration of solution in the solid to liquid ratio was found to be increasing for an increase in adsorbent mass from 0.01 g to 0.04 g. However the q_e/C_e ratio was found to decrease for a further increase in adsorbent mass from 0.04 g to 0.08 g. This observation shows that irrespective of the excess solution concentration available in the solution, the dye sorbed on the solid phase gets decreased for an increase in biosorbent dose from 0.04 g to 0.08 g. Fig. 2(b) also shows the plot of C_e versus q_e and the different operating lines which are generated based on the various biosorbent mass studied in the present investigation. From Fig. 2(b), it is clear that the exponential curve starts only for a biosorbent mass >0.04 g. Thus the reduction in overall surface area of the biosorbent probably because of aggregation during the sorption [6] may be expected for biomass concentration >0.04 g. In addition from Fig. 2(b), the dotted operating line which corresponds to a biomass concentration of 0.08 g crosses the C_e value corresponding to the initial dye concentration of 0.07 g. This suggests that the effect of biomass was nearly the constant for an increasing biomass concentration from 0.07 g to 0.08 g. Thus for a methylene blue dye solution of an initial dye concentration of 100 mg/L, the optimum biosorbent mass which neglects the effect of particle aggregation was found to be 0.04 g/30 mL which is equivalent to 1.33 g of biosorbent/L of dye solution.

3.3. Sorption equilibrium

The experimental equilibrium data of methylene blue onto *P. notatum* were fitted to the three widely used isotherms Freundlich [8], Langmuir [9] and Redlich–Peterson [10] isotherms by non-linear method. For non-linear method, a trial and error procedure, which is applicable to computer operation was developed and used to determine the isotherm parameters by maximizing the respective coefficient of determination, r^2 between the experimental and the isotherms using the *solver* add-in with Microsoft's spreadsheet, Microsoft's Excel. Previously some researcher had found even in the case of non-linear regression, the isotherms parameters was found to get varied during the error minimization process based on the error functions used [11–17]. In the present study in addition to the widely used, r^2, five more error functions namely, The sum of the squares of the error (ERRSQ), the hybrid fractional error function (HYBRID), Marquardt's percent standard deviation (MPSD), the average relative error (ARE), the sum of the absolute errors (EABS) were used to minimize the error distribution between the experimental equilibrium data and predicted isotherms. A spreadsheet was

Table 2
Explanation of different error functions

Error function	Definition/expression	Reference
The sum of the squares of the errors (ERRSQ)	$\sum_{i=1}^{p}(q_{e,calc}-q_{e,isotherm})_i^2$	[11]
The hybrid error function (HYBRID)	$\frac{100}{n-p}\sum_{i=1}^{n}\left[\frac{(q_{e,isotherm}-q_{e,calc})^2}{q_{e,isotherm}}\right]_i$	[11]
Marquardt's percent standard deviation (MPSD)	$100\sqrt{\frac{1}{n-p}\sum_{i=1}^{p}\left(\frac{q_{e,isotherm}-q_{e,calc}}{q_{e,isotherm}}\right)_i^2}$	[11]
The average relative error (ARE)	$\frac{100}{n}\sum_{i=1}^{p}\left|\frac{q_{e,calc}-q_{e,isotherm}}{q_{e,isotherm}}\right|_i$	[11]
The sum of absolute errors (EABS)	$\sum_{i=1}^{p}\left|q_{e,calc}-q_{e,isotherm}\right|_i$	[11]

developed using Microsoft Excel to minimize the error distribution between the experimental data and the predicted isotherms by non-linear regressions method. The error minimization was achieved either by minimizing or maximizing the error function using the *solver* add-in function, Microsoft Excel, Microsoft Corporation. The explanations of various error functions used in the present study are given in Table 2. The Freundlich [8], Langmuir [9] and Redlich–Peterson isotherms [10] were given by the following equations, respectively:

$$q_e = K_F C_e^{1/n} \tag{3}$$

$$q_e = \frac{q_m K_a C_e}{1 + K_a C_e} \tag{4}$$

$$q_e = \frac{A C_e}{1 + B C_e^g} \tag{5}$$

Fig. 3(a)–(c) shows the experimental equilibrium data and the predicted Freundlich, Langmuir and Redlich–Peterson isotherms at 305 K obtained by minimizing/maximizing six different error functions. Fig. 3(a)–(c) also shows the different operating lines generated for various adsorbent mass studied in the present investigation. The calculated isotherm parameters by minimizing the error distribution between experimental data and theoretical isotherms are given in Table 3. From Fig. 3(a) and (c), it is observed that irrespective of the error functions used, the predicted theoretical isotherm remains more or less equal. However in the case of three parameter isotherm, the Redlich–Peterson isotherm (Fig. 3(c)), it can be observed that the predicted isotherm by maximizing the r^2-values exhibits a Langmuir type isotherm whereas the other error functions failed to better represent the monolayer saturation. From Table 3, it can be observed that in the case of ERRSQ, HYBRID, MPSD, ARE and EABS it is observed that the Redlich–Peterson isotherm constants A and B are not much greater than 1 thus suggesting that isotherm is not following the Freundlich isotherm [18]. In addition from Table 1, it was observed that the g values are not equal to zero thus confirming that there does not exist a linear (Henry's) relation between C_e and q_e. In the case of r^2, it is observed that the g values were unity and the B values were less than unity. The value of g equal to unity suggests the isotherm is approaching the Langmuir but not the Freundlich. Thus in the case of three parameters Redlich–Peterson isotherm, it is more important to consider the value of A and B in addition to the value of the r^2. Fig. 3(d) shows the experimental equilibrium data and the predicted Langmuir and Redlich–Peterson isotherms by maximizing the r^2 function. From Fig. 3(d), it is observed that Redlich–Peterson isotherm exactly overlapped the Langmuir isotherm with the same r^2-value (Table 3). The error functions other than r^2-value does not show any relation between the Freundlich and Redlich–Peterson isotherm or any relation between Langmuir isotherm or Redlich–Peterson isotherm (not
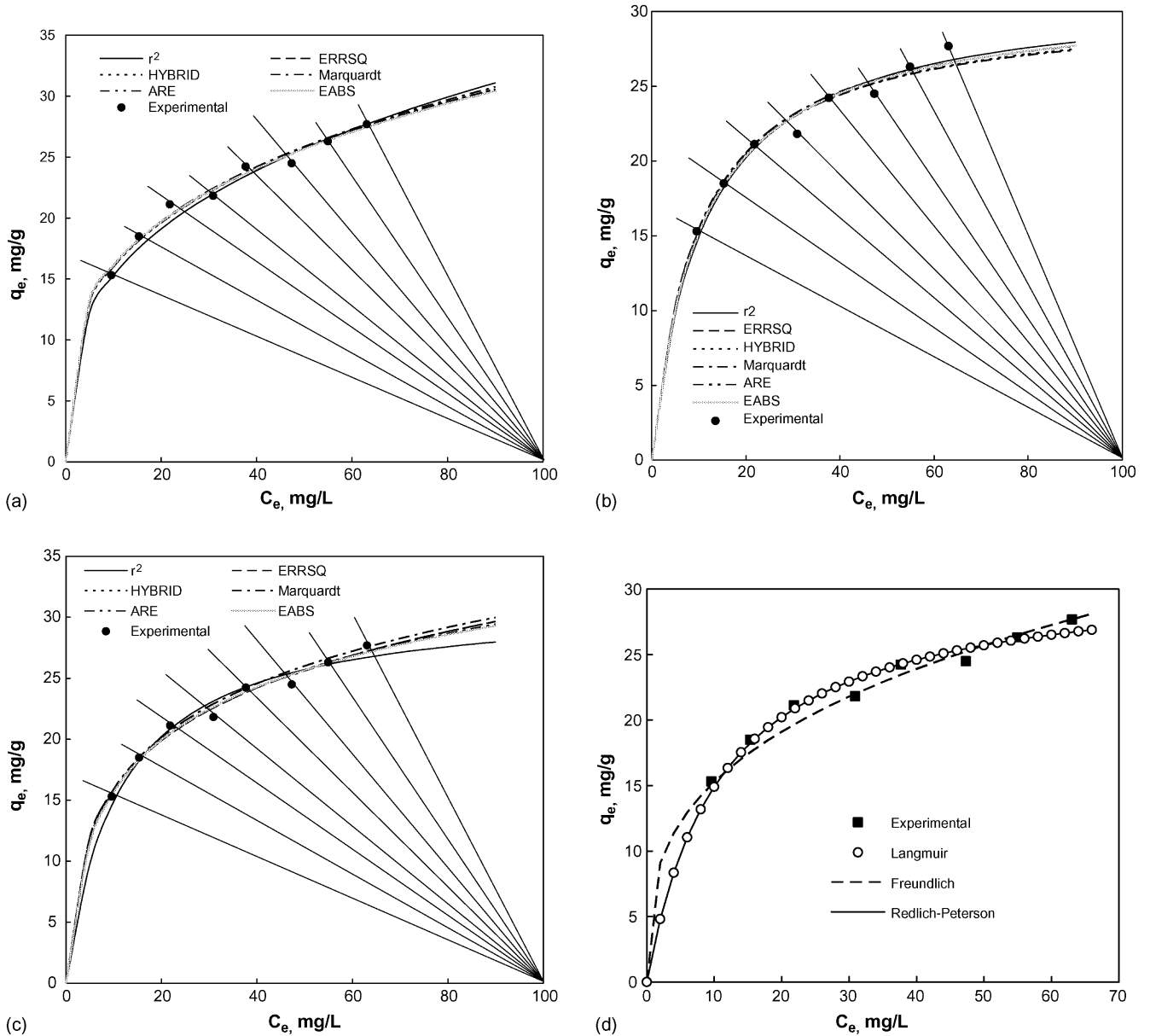
Table 3
Isotherm constants for the sorption of methylene blue onto *P. notatum*

Isotherm	r^2	ERRSQ	HYBRID	MPSD	ARE	EABS
Langmuir						
q_m	31.40314	30.93706	30.50378	30.74538	30.41728	30.93688
K_L	0.090402	0.095793	0.101379	0.100701	0.101941	0.095795
MEF[a]	0.967388	0.516412	0.546467	0.009045	0.144041	0.516412
Freundlich						
K_F	7.247803	8.301829	8.129205	8.140677	8.101327	8.30165
$1/n$	0.323558	0.288561	0.294486	0.295386	0.295177	0.288567
MEF[a]	0.969338	0.320256	0.439058	0.009583	0.113364	0.320256
Redlich–Peterson						
A	2.838942	7.965873	7.160207	6.982718	6.538389	5.644515
B	0.090404	0.647377	0.558669	0.529458	0.482674	0.381726
g	1	0.795122	0.803217	0.80655	0.816163	0.834753
MEF[a]	0.967388	0.276639	0.321355	0.007897	0.083292	0.286837
Redlich–Peterson						
A		7.962573	6.653507	6.981443	6.178652	6.443923
B		0.646993	0.497092	0.525349	0.439522	0.473297
g		0.795161	0.813204	0.809324	0.82449	0.816762
MEF[a]		0.276639	0.317953	0.007904	0.083147	0.280012

[a] Minimized/maximized error function.

Fig. 3. Experimental equilibrium data and (a) Freundlich, (b) Langmuir, (c) Redlich–Peterson and (d) predicted isotherms by maximizing r^2 for the sorption of methylene blue onto *P. notatum* (*V/M*, 0.05 L/0.05 g).

shown). From Table 3, it is observed that only r^2-value produces the *g* value equal to unity and in the case of other error functions the value of *g* lies in the range of 0.79–0.83. In order to check the ability of the other error functions in minimizing the error distribution between the experimental and predicted isotherms within the theoretical limit for the constant $0 < g < 1$, a spreadsheet was developed to solve the Redlich–Peterson isotherm without considering the theoretical limits. Table 3 shows the predicted Redlich–Peterson isotherm constants and the corresponding error functions obtained by minimizing the error functions other than r^2. From Table 3, it was observed that the value of *g* obtained without considering the theoretical limits of Redlich–Peterson isotherm remains more or less same with respect to the predicted Redlich–Peterson isotherm, which was obtained by iteration technique subjected under the theoretical limits. This clearly

indicates that the error functions ERRSQ, HYBRID, MPSD, ARE and EABS does not take any much effort in considering the theoretical limits of Redlich–Peterson isotherm. This can be observed from the value of *g* obtained after 500 iterations performed using the *solver* add-in function, Microsoft Excel, Microsoft Corporation. The present study makes clear that r^2 may be an appropriate error function to predict the three parameter theoretical (Redlich–Peterson) isotherm. However there is no problem while using the r^2 or other error functions while predicting the two parameter theoretical isotherms namely Freundlich and Langmuir. Another important conclusion which can be made from Table 3 is, for both the case of two parameter and three parameter isotherm, r^2, MPSD and ARE provided a minimum error distribution (Table 3) between the isotherm and the experimental data. In addition from Table 1, it can be noted

Table 4
Sorption capacity of low cost sorbents for methylene uptake

Adsorbent	q_m (mg/g)	Reference
Fe(III)/Cr(III) hydroxide	22.8	[19]
Chelating polymer	30	[20]
Biogas residual slurry	1.465	[21]
Fly ash	5.718	[5]
Coir pith carbon	5.87	[22]
Saw dust	32.26	[23]
Raw clay	27.49	[24]
Calcined clay	13.44	[24]
Neem leaf powder	8.76	[25]
Egg shell	<1	[26]

that ERRSQ and EABS equally minimizes the error distribution structure between the experimental and predicted isotherms and also produced the same isotherm constants (Table 3). Based on the r^2-value and also based on the predicted Redlich–Peterson isotherm constant A, B and g, it can be concluded that both Langmuir and Redlich–Peterson isotherm well represents the equilibrium uptake of methylene blue by *P. notatum*. In addition the higher monolayer sorption capacity, q_m value of 31 mg/g suggests that the low cost biosorbent *P. notatum* can be used as a sorbent material for the removal of methylene blue from their aqueous solutions. A comparison of other low cost adsorbents with the *P. notatum* for the equilibrium uptake of methylene blue was given in Table 4. From Table 4, it can be observed that *P. notatum* is competitive to other low cost sorbents for the uptake of methylene blue from their aqueous solutions. Irrespective of the predictions from the isotherm constants or the error functions, there exist a common observation in Fig. 3(a)–(c). Fig. 3(a)–(c) shows the operating lines generated corresponding to various sorbent dosages. From Fig. 3(a)–(c), it can be observed that all the three isotherms, for all the operating lines studied showed a more or less similar amount of equilibrium dye concentration while treating methylene blue solution of initial dye concentration of 100 mg/L. This suggests that any isotherm constants obtained by minimizing or maximizing the error functions can be useful in designing the batch sorber system.

3.4. Biosorption kinetics

Fig. 4 shows the effect of initial dye concentration on the rate of dye uptake for methylene blue onto *P. notatum*. From Fig. 4, it was observed that the amount of dye adsorbed gets increased with increasing initial dye concentration and contact time. From Fig. 4, it also observed that the rate of dye uptake was found to be very rapid for the initial contact period of 6 min and thereafter the dye uptake process tends to proceed at a very slower rate and finally reaches saturation. The saturation time was found to be 30 min irrespective of the initial methylene blue concentration. The effect of initial dye concentration on the dye uptake rate were shown in Fig. 5. The term r in Fig. 5 represents the ratio of dye uptake to the contact time interval. Using the experimental data, the rate of dye uptake in the initial rapid phase and the later slower phase was calculated using the sim-
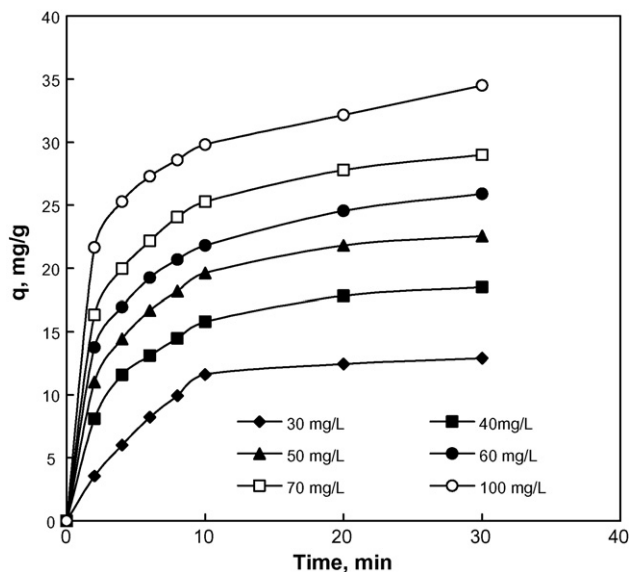

Fig. 4. Adsorption kinetics for the sorption of methylene blue onto *P. notatum* (*V/M*, 2 L/2.67 g; pH 8).

ple rate expression $r = dC/dt$ by differential method. From the rate shown in Fig. 5, it can be observed that the rate of dye uptake in the initial rapid phase is roughly 10 times greater than the rate of dye uptake in the slower phase. From Fig. 5, it was observed that the rate of dye uptake in the initial rapid phase, $r_{\text{Rapid phase}}$, was found to be increasing as 1.37, 2.19, 2.78, 3.21, 3.69 and 4.54 mg/(g min) for an initial dye concentration of 30, 40, 50, 60, 70 and 100 mg/L, respectively. Similarly the rate of dye uptake for the slower phase, $r_{\text{Slower phase}}$, were found to increasing as 0.19, 0.22, 0.25, 0.28 and 0.30 mg/(g min) for an initial dye concentration of 30, 40, 50, 60, 70 and 100 mg/L, respectively. The rate of methylene blue uptake by *P. notatum* for different initial dye concentration fits the following equations for the initial rapid phase and the later slower phase,
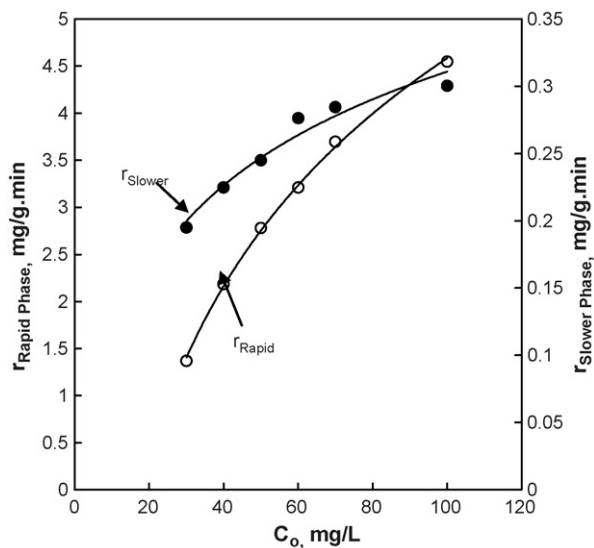

Fig. 5. Effect of initial dye concentration on the rate of methylene blue adsorption by *P. notatum* (*V/M*, 2 L/2.67 g; pH 8).
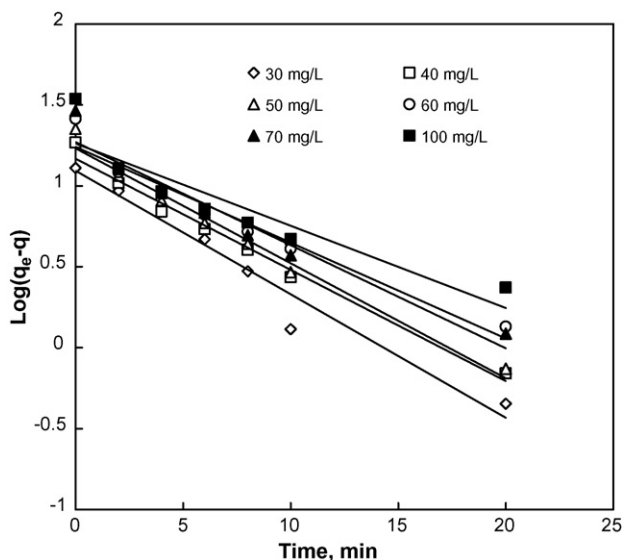
Fig. 6. Pseudo first order kinetics for the sorption of methylene blue onto *P. notatum* (*V/M*, 2 L/2.67 g; pH 8).

Fig. 7. Pseudo second order kinetics for the sorption of methylene blue onto *P. notatum* (*V/M*, 2 L/2.67 g; pH 8).

respectively:

$$r_{\text{Rapid phase}} = 2.6422 \ln(C_0) - 7.5825; \qquad r^2 = 0.9989 \quad (6)$$

$$r_{\text{Slower phase}} = 0.0923 \ln(C_0) - 0.1142; \qquad r^2 = 0.957 \quad (7)$$

The transient behavior of methylene blue uptake by *P. notatum* following the pseudo first order [27] and pseudo second order kinetics [28,29] can be represented by the following equations:

$$\frac{dq}{dt} = k_1(q_e - q) \tag{8}$$

$$\frac{dq}{dt} = k_2(q_e - q)^2 \tag{9}$$

Integrating Eqs. (8) and (9) with respect to the limits, $q = 0$ at time $t = 0$ and $q = q$ at time $t = t$, the simplified linear expression of first order and second order expressions can be given by the following equations, respectively:

$$\log(q_e - q) = \log(q_e) - \frac{k_1 t}{2.303} \tag{10}$$

$$\frac{t}{q} = \frac{1}{k_2 q_e^2} + \frac{t}{q_e} \tag{11}$$

Thus the kinetics of methylene blue sorption onto *P. notatum* following the pseudo first order and pseudo second order kinetic process can be analyzed from the plot of $\log(q_e - q)$ versus t and t/q versus t, respectively.

Figs. 6 and 7 show the pseudo first order kinetics and pseudo second order kinetic plot for the sorption of methylene blue onto *P. notatum*. The pseudo first order kinetic constant, k_1 (min^{-1}), and the amount of dye adsorbed at equilibrium, q_e (mg/g), can be calculated from the slope of Figs. 6 and 7 using Eqs. (10) and (11), respectively. Similarly the pseudo second order kinetic constant, k_2 (g/(mg min)), and the amount of dye adsorbed at equilibrium, q_e (mg/g), can be calculated from the intercept and

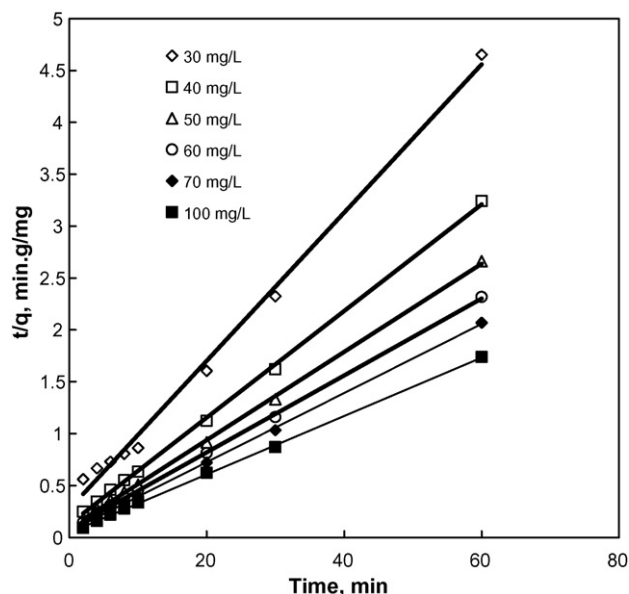slope of the plot between t/q versus t using Eq. (11). The calculated kinetic constants, k_1, k_2 and the theoretically predicted q_e and the corresponding r^2-values were shown in Table 5.

From Table 5, the relatively lower r^2-value for a pseudo first order kinetics than the r^2-value for pseudo second order kinetics suggests that pseudo second order expression as the best fit kinetic expression. Though the r^2-value in the range of 0.96 is acceptable to argue as a best fit, this model fails to explain the sorption saturation. According to the Lagergren pseudo first order kinetics as given in Eq. (10), the intercept of the Lagergren kinetic plot should theoretically represent the adsorption saturation for the given condition. In the present study, from Table 5, it can be observed that the q_e values predicted using the Lagergren plot fails to predict the q_e value for all the initial dye concentration studied. This conforms that it is not wise to use this model in predicting the sorption kinetics of methylene blue uptake by *P. notatum* particles. Thus it is very important to select the best fit kinetics based on how well the theory of sorption kinetics was explained and also based on the r^2-value. The relatively higher r^2-value (>0.99) for pseudo second order kinetics suggested the sorption of methylene blue onto *P. notatum* follows a pseudo second order kinetics. In addition from Table 5, it was observed that the theoretically predicted q_e values were found to be agreeing with the experimental q_e values. This confirms the applicability of the pseudo second order kinetic model in predicting the amount of dye sorbed at equilibrium. Though the higher r^2-value for pseudo second order kinetics suggested that the methylene blue uptake by *P. notatum* follows a pseudo second order kinetics, there does not exist a definite relation between the initial dye concentration and the reaction rate constant, k_2. Previously most of the studies reported a decrease in k_2 with increasing initial solute concentration. Ho et al. [30] reported that the second order rate constant, k_2 was found to decrease with increasing initial dye concentration for the sorption of acid blue 9 onto activated clay. A similar observation was reported for the sorption of acid

Table 5
Kinetic constants and mass transfer coefficients for the sorption of methylene blue onto *P. notatum*

C_0 (mg/L)	q_e experimental (mg/g)	Pseudo first order kinetics			Pseudo second order kinetics			k_i (mg/ (g min$^{0.5}$))	K_s (cm/s)	B	D_i (cm^2/s)
		k_1 (min^{-1})	q_e (mg/g)	r^2	k_2 (g/ (mg min))	q_e (mg/g)	r^2				
30	12.9	0.175719	12.35947	0.9627	0.018384	14.0056	0.9944	0.565881	7.01275E−06	0.1555	9.86E−06
40	18.5025	0.158216	14.69941	0.9859	0.020464	19.45525	0.9992	1.194506	6.96456E−06	0.1412	8.95E−06
50	22.55	0.163513	17.03727	0.9812	0.019562	23.58491	0.9994	1.281263	6.95974E−06	0.1472	9.33E−06
60	25.89	0.136338	17.03727	0.951	0.016985	27.02703	0.9995	1.778345	6.8039E−06	0.1205	7.64E−06
70	29	0.146701	18.62945	0.9456	0.018211	30.003	0.9997	1.621842	6.8716E−06	0.1312	8.32E−06
100	34.5	0.116992	16.03245	0.8424	0.016588	35.58719	0.9996	2.014137	6.09218E−06	0.1022	6.48E−06

blue 9 by a mixture of activated carbon and activated clay sorbent [31], sorption of basic red 18 by activated clay [29], acid blue 25 by peat particles [32], acid blue 25 by wood particles [32] and lead ions sorption onto peat particles [33]. Previously some studies showed an increasing trend in k_2 value with respect to increasing initial dye concentration for the sorption of safranin onto activated carbon [34]. Most of the literature information shows that irrespective of the trend between the pseudo second order rate constant, k_2 and the initial dye concentration, the k_2 values were found to be increasing and then decreasing and again increasing for an continuous increase in the initial dye concentration. Sorption of basic red 18 by activated clay [29] showed some rise and fall in k_2 values for an increase in initial dye concentration. This behavior cannot be justified statistically. Any how irrespective of the rise and fall in the k_2 values with initial dye concentration, there always exist a definite trend between the initial dye concentration and the pseudo second order rate constant, k_2. For most of the sorption systems irrespective of the increase or decrease in k_2 values with respect to initial dye concentration, there exist an acceptable trend between the initial dye concentration and in most of the cases reported, the trend was a decreasing k_2 with increasing initial dye concentration. In the present study, though there is an increase and decrease in k_2 values with increasing initial dye concentration. However there is a definite trend which suggests that the pseudo second order rate constant, k_2 values gets decreased with increasing initial dye concentration. This observation suggests for most of the cases there exist an inverse trend between the initial dye concentration and the second order rate constant k_2, which also agrees with the present study. Our previous study showed that a different linear form of pseudo second order expression provided different relation between the initial dye concentration and rate constant [34]. Based on the way the kinetics is linearized the value of k_2 changes for the range of initial dye concentration. These observations suggested the mathematical complexities in the process of search for best fit kinetics. Irrespective of the difficulties in using regression techniques search for best fit kinetics is a viable technique to design the sorption systems because most of the semi-empirical kinetic expressions very well represents the sorption systems for the range of operating variables studied. Since there is a rise and fall in k_2 value with initial dye concentrations, simple correlations were developed between the initial dye concentration and the parameters involved in the pseudo second order kinetic expression. The correlation between C_0 and

k_2 and C_0 and q_e are given in the following equations with an r^2-value of 0.9842 and 0.9982, respectively:

$$k_2 = \frac{C_0}{33.23C_0^{1.1244}} \tag{12}$$

$$q_e = 18.096\ln(C_0) - 47.286 \tag{13}$$

Eqs. (12) and (13) were substituted in the pseudo second order expression to get a generalized kinetic expression that predicts the dye uptake kinetics for the range of initial dye concentration studied. The generalized pseudo second order expression obtained using Eqs. (12) and (13) is given by:

$$q = \frac{(C_0/33.233C_0^{1.1244})[18.096\ln(C_o) - 47.286]t}{1 + \{(C_0/33.233C_0^{1.1244})[18.096\ln(C_0) - 47.286]^2\}t} \tag{14}$$

Eq. (14) can be used to predict the sorption kinetics of methylene blue uptake by *P. notatum* particles. Fig. 8 shows the predicted pseudo second order kinetics for the range of initial dye concentrations studied. Fig. 8 also shows some of the experimental kinetic data. From Fig. 8, it is clearly observed that the pseudo second order expressions can be used to predict the dye uptake kinetics by *P. notatum* particles. Fig. 8 also make clear that the pseudo second order kinetics predicted using Eq. (14) well represents the experimental kinetic data. This suggests the applicability of correlations as in Eqs. (12) and (13) and also shows the applicability of the predicted pseudo second order kinetic constants. The important point to be noticed in this study is, it is better to perform kinetic experiments for different initial dye concentrations while analyzing a kinetic model. In addition it is always better to check the accuracy of predicted kinetic constants of the best fit kinetic expression in predicting the kinetics of the experimental data. Another important point that can be concluded in the present study is, if there is no definite relation between kinetic constant and the initial dye concentration, it is better to perform experiments at different initial dye concentrations in order fond the generalized trend between the rate constant and the initial dye concentration. A further observation from this exercise is that the rate coefficients of the semi-empirical kinetic expression should be properly correlated with major systems variables studies. Previously Azizian and Yahyaei [35] had made a similar conclusion that one should not do kinetic experiments at only once initial dye concentration and it is better to do experiments at different initial dye concen-
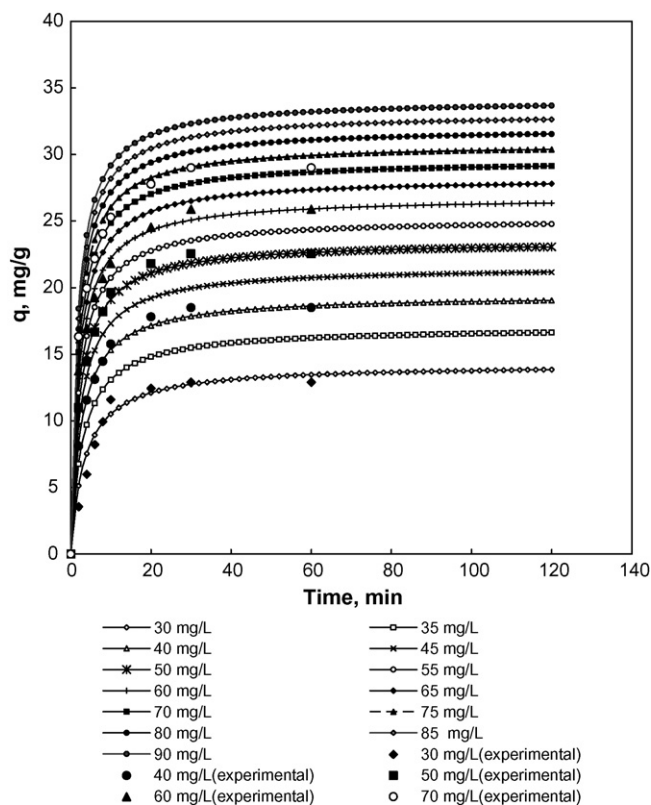
Fig. 8. Experimental data and simulated kinetics using Eq. (14) for various initial dye concentrations.

trations. In this study the statement of the Azizian and Yahyaei [35] is validated with the help of simulated pseudo second order kinetics for the studied system.

3.5. Biosorption mechanism

From a mechanistic viewpoint to interpret the experimental data, it is necessary to identify the steps involved during adsorption described by external mass transfer (boundary layer diffusion) and intraparticle diffusion [36]. The different mechanism involved in the methylene blue uptake by *P. notatum* can be analyzed from the intraparticle diffusion [37] plot of q versus $t^{0.5}$. Previous studies by various researchers showed that the plot of q versus $t^{0.5}$ represents multilinearity, which characterizes the two or more steps involved in the sorption process [38–41]. The slope of different linear portions of the Weber Morris plot will characterize the limiting mechanism due to pore diffusion in the overall adsorption process. According to Weber and Morris [37], an intraparticle diffusion coefficient k_i is given by:

$$k_i = \frac{q}{t^{0.5}} \qquad (15)$$

Thus the k_i ($mg/(g\,min^{0.5})$) value can be obtained from the slope of the plot of q (mg/g) versus $t^{0.5}$ ($min^{0.5}$). Fig. 9 shows the plot of q versus $t^{0.5}$ for methylene blue onto *P. notatum* particles. From Fig. 9, it was noted that the sorption process tends to be followed by two phases. It was found that the linear portion ended with a smooth curve followed by a linear portion.
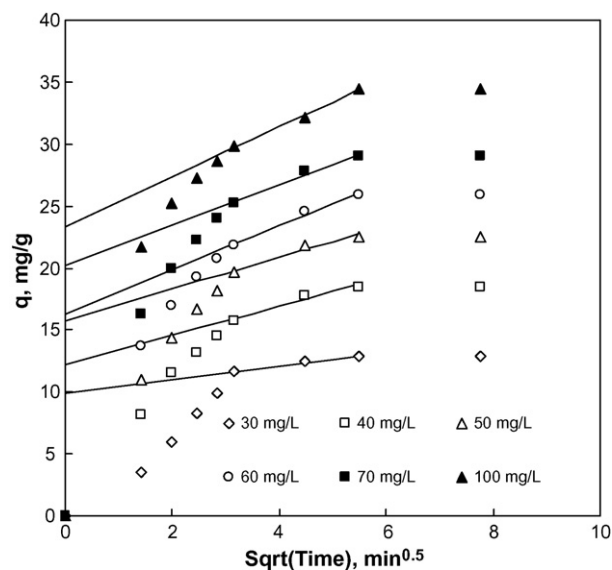

Fig. 9. Intraparticle diffusion kinetics for the sorption of methylene blue onto *P. notatum* (V/M, 2 L/2.67 g; pH 8).

A similar type of pattern was reported for the sorption of basic dyes onto peat particles [41], methylene blue onto fly ash [5], methylene blue onto mango seed kernel particles [39]. The two phases in the intraparticle diffusion plot suggest that the sorption process proceeds by surface sorption and intraparticle diffusion. The initial curved portion of the plot indicates a boundary layer effect while the second linear portion is due to intraparticle or pore diffusion. The slope of the second linear portion of the plot has been defined as the intraparticle diffusion parameter k_i ($mg/(g\,min^{0.5})$). On the other hand, the intercept of the plot reflects the boundary layer effect. The larger the intercept, the greater the contribution of the surface sorption in the rate limiting step [42]. The calculated intraparticle diffusion coefficient at different initial dye concentration was given in Table 5.

From design aspect, it is important to estimate which is the rate-limiting step (pore or surface diffusion) involved in the sorption process. Thus the kinetic data have been analyzed using the model of Boyd et al. [43] and Reichenberg [44]:

$$Bt = -0.4977 - \ln(1 - F) \qquad (16)$$

$$Bt = 6.28318 - 3.2899F - 6.28318(1 - 1.0470F)^{1/2} \qquad (17)$$

where F is a mathematical function of Bt and vice versa. B is given by:

$$B = \frac{\Pi^2 D_i}{r^2} \qquad (18)$$

where D_i is the effective diffusion coefficient.

Eqs. (16) and (17) was proposed based on the assumption of particle diffusion as the sole rate controlling process. Eqs. (16) and (17) are used to calculate Bt values at different time, t. Eq. (16) was used to calculate Bt values for F value greater than 0.85 and Eq. (17) was used to calculate Bt values for F less than 0.85. The calculated Bt values were plotted against time, t, as shown in Fig. 10. The linearity in the plot is used to distinguish whether external or intraparticle transport controls the
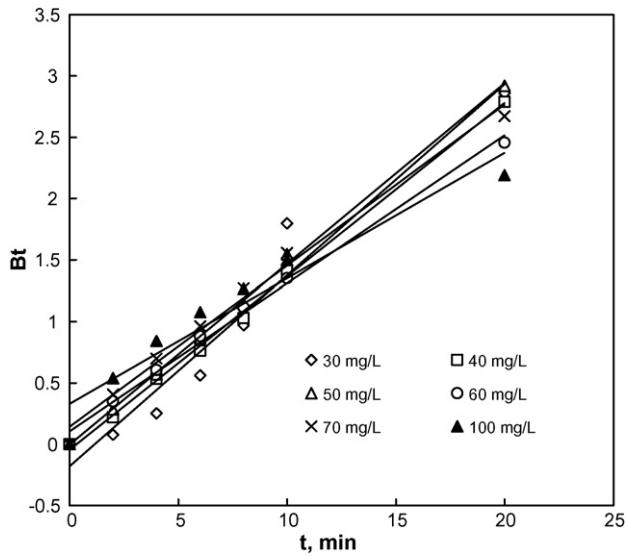
Fig. 10. Boyd plot for methylene blue onto *P. notatum*.

Fig. 11. Effect of external mass transfer on initial dye concentration for the sorption of methylene blue onto *P. notatum*.

adsorption rate. From Fig. 10, it was observed that the relation between Bt and t was linear at all dye concentrations but does not pass through origin, confirming that surface diffusion is the rate-limiting step [5,38,39,43,44]. The calculated B values were used to calculate the effective diffusion coefficient, D_i (cm²/s) using Eq. (18), where r represents the radius of the particle calculated by sieve analysis and by assuming as spherical particles. The calculated D_i values at different initial dye concentrations were given in Table 5. The average D_i values were estimated to be 8.42×10^{-6} cm²/s.

As the Boyd plot confirms surface diffusion as the rate controlling step, the rate constant corresponding to external mass transfer of methylene blue onto *P. notatum* was calculated using the external mass transfer model proposed by Furusawa and Smith [45]. The experimental data are analyzed assuming a three-step model:

(1) mass transfer of methylene blue from bulk liquid to particle;
(2) intraparticle diffusion;
(3) adsorption at internal site.

It is assumed that third step is rapid when compared to the first two steps [45]. In a fully agitated solid/liquid adsorber, mixing in the liquid is very rapid. Thus the concentration of sorbate and sorbent within the adsorber system are nearly uniform. Thus the change in concentration of sorbate with respect to the time is related by the following equation [46]:

$$-\frac{dC}{dt} = K_s S(C - C_e) \tag{19}$$

where S is the surface area of adsorbent per unit volume of particle slurry and is given by:

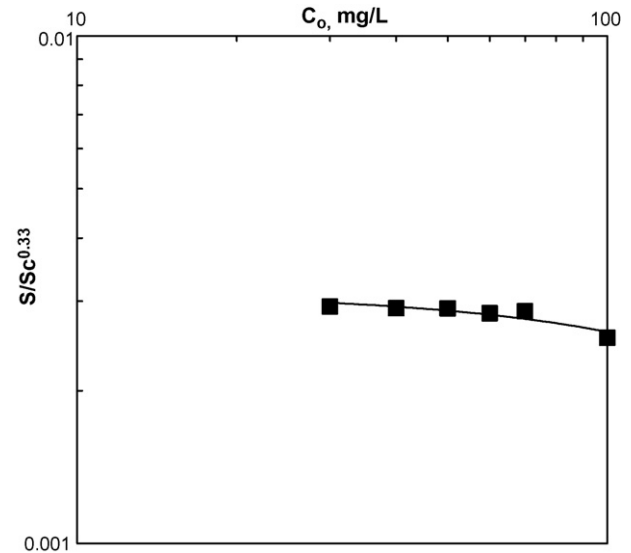$$S = \frac{6M}{Vd_p\rho(1 - \varepsilon_p)} \tag{20}$$

At time $t = 0$, $C_e = 0$, thus the Eq. (20) becomes:

$$\left[\frac{d(C/C_0)}{dt}\right]_{t=0} = -K_s S \tag{21}$$

The external mass transfer coefficient K_s can be calculated from the slope of C/C_0 versus time t using Eq. (21). The calculated external mass transfer coefficient, K_s (cm/s), at different initial dye concentrations for the sorption of methylene blue onto *P. notatum* was given in Table 5. The calculated external mass transfer coefficients were represented in the form of dimensionless mass transfer numbers ($Sh/Sc^{0.33}$). The effect of initial dye concentration on dimensionless mass transfer numbers were shown in Fig. 11. The experimental data in Fig. 11 fits the generalized expression:

$$\frac{Sh}{Sc^{0.33}} = (C_0)^{-5 \times 10^{-6}} \tag{22}$$

From Fig. 11, it was observed that the mass transfer was found to get decreased with increasing initial dye concentration. Where the Sh and Sc represents the Sherwood and Schmidt numbers and is given by the following equations:

$$Sh = \frac{\beta d_p}{D_{AB}} \tag{23}$$

$$Sc = \frac{\upsilon}{D_{AB}} \tag{24}$$

where D_{AB} represents the diffusivity of dyes in solvent (water) and can be calculated using Wilke–Chang expression [46]:

$$D_{AB} = \frac{7.4 \times 10^{-8}(\Phi M_B)^{1/2}T}{\mu_B V_A^{0.6}} \tag{25}$$

4. Conclusions

The present study showed that the biosorbent *P. notatum* can be used as a potential sorbent for the removal of methylene blue

from their aqueous solutions. The amount of dye sorbed was found to be increasing with increasing initial solution pH for the sorption of methylene blue onto *P. notatum*. The amount of dye uptake (mg/g) was found to increase with increase in dye concentration and contact time and found to decrease with increase in *P. notatum* mass. The kinetics of methylene blue uptake by *P. notatum* was found to follow a pseudo second order kinetic expression. Equilibrium data of methylene blue onto *P. notatum* was found to follow Langmuir isotherm thus suggesting the monolayer sorption of dye ions. Redlich–Peterson was found to be a special case of Langmuir when the constant *g* equals unity. Error minimization with different error functions suggests that r^2 minimizes the error distribution between the experimental data and both the two and three parameter isotherms. In addition, the error functions ERRSQ, HYBRID, MPSD, ARE and EABS predicts the two parameter isotherms very well however these error functions doesn't obey the theory of Redlich–Peterson isotherm during the error minimization process. The overall kinetics of methylene blue uptake by *P. notatum* was found to follow a pseudo second order kinetics. A Boyd plot confirms the external mass transfer as the slowest step involved in the sorption process. The effect of initial dye concentration on the external mass transfer was represented in the form of dimensionless mass transfer numbers ($Sh/Sc^{0.33}$).

Acknowledgments

References

[1] T. Robinson, B. Chandran, P. Nigam, Removal of dyes from an artificial textile dye effluent by two agricultural waste residues, corncob and barley husk, Environ. Int. 28 (2002) 29–33.

[2] E. Forgacs, T. Cserháti, G. Oros, Removal of synthetic dyes from wastewaters: a review, Environ. Int. 30 (2004) 953–971.

[3] E. Weber, N.L. Wolfe, Kinetics studies of reduction of aromatic azo compounds in anaerobic sediment/water systems, Environ. Toxicol. Chem. 6 (1987) 911–920.

[4] M.M. Figueria, B. Volesky, K. Azarian, V.S.T. Ciminelli, Biosorption column performance with a metal mixture, Environ. Sci. Technol. 34 (2000) 4320–4326.

[5] K.V. Kumar, V. Ramamurthi, S. Sivanesan, Modeling the mechanism involved during the sorption of methylene blue onto fly ash, J. Colloid Interf. Sci. 284 (2005) 14–21.

[6] Y. Nuhoglu, E. Malkoc, A. Gürses, N. Canpolat, The removal of Cu(II) from aqueous solutions by *Ulothrix zonata*, Bioresour. Technol. 85 (2005) 331–333.

[7] G.C. Dönmez, Z. Aksu, A. Özturk, A comparative study on heavy metal biosorption characteristics of some algae, Process Biochem. 34 (1999) 885–892.

[8] H.M.F. Freundlich, Over the adsorption in solution, Z. Phys. Chem. 57A (1906) 385–470.

[9] I. Langmuir, The constitution and fundamental properties of solids and liquids, J. Am. Chem. Soc. 38 (1916) 2221–2295.

[10] O. Redlich, D.L. Peterson, A useful adsorption isotherm, J. Phys. Chem. 63 (1959) 1024.

[11] J.C.Y. Ng, W.H. Cheung, G. McKay, Equilibrium studies of the sorption of Cu(II) ions onto chitosan, J. Colloid Interf. Sci. 255 (2002) 64–74.

[12] Y.C. Wong, Y.S. Szeto, W.H. Cheung, G. McKay, Adsorption of acid dyes on chitosan-equilibrium isotherm analyses, Process Biochem. 39 (2004) 693–702.

[13] Y.S. Ho, W.T. Chiu, C.C. Wang, Regression analysis for the sorption isotherms of basic dyes on sugarcane dust, Bioresour. Technol. 96 (2005) 1285–1291.

[14] I.D. Mall, V.C. Srivastava, N.K. Agarwal, I.M. Mishra, Removal of congo red from aqueous solution by bagasse fly ash and activated carbon: kinetic study and equilibrium isotherm analyses, Chemosphere 61 (2005) 492–501.

[15] J.F. Porter, G. McKay, K.H. Choy, The prediction of sorption from a binary mixture of acidic dyes using single- and mixed-isotherm variants of the ideal adsorbed solute theory, Chem. Eng. Sci. 54 (1999) 5863–5885.

[16] Y.S. Ho, J.F. Porter, G. McKay, Equilibrium isotherm studies for the sorption of divalent metal ions onto peat: copper, nickel and lead single component systems, Water Air Soil Pollut. 141 (2002) 1–33.

[17] S. Kundu, A.K. Gupta, Arsenic adsorption onto iron oxide-coated cement (IOCC): regression analysis of equilibrium data with several isotherm models and their optimization, Chem. Eng. J. 122 (2006) 93–106.

[18] K.V. Kumar, Selection of optimum isotherm and kinetics, Ph.D. Thesis, Anna University, 2006.

[19] C. Namasivayam, S. Sumithra, Removal of direct red 12B and methylene blue from water by adsorption onto Fe(III)/Cr(III) hydroxide, an industrial solid waste, J. Environ. Manage. 74 (3) (2005) 207–215.

[20] G. Annadurai, Adsorption of basic dye on strongly chelating polymer: batch kinetics studies, Iran. Polym. J. 2 (4) (2002) 237–244.

[21] C. Namasivayam, R.T. Yamuna, Utilizing biogas residual slurry for dye adsorption, Am. Dyestuff Reporter August (1994) 23–27.

[22] D. Kavitha, C. Namasivayam, Experimental and kinetic studies on methylene blue adsorption by coir pith carbon, Bioresour. Technol. 98 (2007) 14–21.

[23] D.S. De, J.K. Basu, Adsorption of methylene blue on to a low cost adsorbent developed from saw dust, Indian J. Environ. Prot. 19 (1998) 416–421.

[24] D. Ghosh, K.G. Bhattacharyya, Removing colour from aqueous medium by sorption on natural clay: a study with methylene blue, Indian J. Environ. Prot. 21 (2001) 903–910.

[25] K.G. Bhattacharyya, A. Sharma, Kinetics and thermodynamics of Methylene Blue adsorption on Neem (*Azadirachta indica*) leaf powder, Dyes Pigments 65 (2005) 51–59.

[26] W.T. Tsai, J.M. Yang, C.W. Lai, Y.H. Cheng, C.C. Lin, C.W. Yeh, Characterization and adsorption properties of eggshells and eggshell membrane, Bioresour. Technol. 97 (2006) 488–493.

[27] Y.S. Ho, Citation review of Lagergren kinetic rate equation on adsorption reactions, Scientometrics 59 (1) (2004) 171–177.

[28] G. Blanchard, M. Maunaye, G. Martin, Removal of heavy metals from waters by means of natural zeolites, Water Res. 18 (1984) 1501–1507.

[29] Y.S. Ho, Pseudo-isotherms using a second order kinetic expression constant, adsorption, Adsorption 10 (2004) 151–158.

[30] Y.S. Ho, C.C. Chiang, Y.C. Hsu, Sorption kinetics for dye removal from aqueous solution using activated clay, Sep. Sci. Technol. 36 (2001) 2473–2488.

[31] Y.S. Ho, C.C. Chiang, Sorption studies of acid dye by mixed sorbents, Adsorption 7 (2001) 139–147.

[32] Y.S. Ho, G. McKay, A two stage batch sorption optimized design for dye removal to minimize contact time, Trans. IChemE 76B (1998) 313–318.

[33] Y.S. Ho, G. McKay, A multistagesorption design with experimental data, Adsorb. Sci. Technol. 17 (1999) 233–243.

[34] K.V. Kumar, Pseudo-second order models for the adsorption of safranin onto activated carbon: comparison of linear and non-linear regression methods, J. Hazard. Mater. 142 (2007) 564–567.

[35] S. Azizian, B. Yahyaei, Adsorption of 18-crown-6 from aqueous solution on granular activated carbon: a kinetic modeling study, J. Colloid Interf. Sci. 299 (2006) 112–115.

[36] M. Sarkar, P.K. Acharya, B. Bhattacharya, Modeling the adsorption kinetics of some priority organic pollutants in water from diffusion and activation energy parameters, J. Colloid Interf. Sci. 266 (2003) 28–32.

[37] W.J. Weber Jr., J.C. Morris, Kinetics of adsorption on carbon from solution, J. Sanit. Eng. Div. Am. Soc. Civ. Eng. 89 (1963) 31–60.

[38] V. Vadivelan, K.V. Kumar, Equilibrium, kinetics, mechanism, and process design for the sorption of methylene blue onto rice husk, J. Colloid Interf. Sci. 286 (2005) 90–100.

[39] K.V. Kumar, A. Kumaran, Removal of methylene blue by mango seed kernel powder, Biochem. Eng. J. 27 (2005) 83–93.

[40] Y.S. Ho, G. McKay, Sorption of dyes and copper ions onto biosorbents, Process Biochem. 38 (2003) 1047–1061.

[41] Y.S. Ho, G. McKay, The kinetics of sorption of basic dyes from aqueous solution by sphagnum moss peat, Can. J. Chem. Eng. 76 (1998) 822–827.

[42] M. Sankar, G. Sekaran, S. Sadulla, T. Ramasami, Removal of diazo and triphenylmethane dyes from aqueous solutions through an adsorption process, J. Chem. Technol. Biotechnol. 74 (1999) 337–344.

[43] G.E. Boyd, A.W. Adamsom, L.S. Myers Jr., The exchange adsorption of ions from aqueous solutions by organic zeolites. I. Ion-exchange equilibria, J. Am. Chem. Soc. 69 (1947) 2836–2848.

[44] D.J. Reichenberg, Properties of ion exchange resins in relation to their structure. III. Kinetics of exchange, Am. Chem. Soc. 75 (1953) 589–597.

[45] T. Furusawa, J.M. Smith, Fluid-particle and intraparticle mass transport rates in slurries, Ind. Eng. Chem. Fundam. 12 (2) (1973) 197–203.

[46] C.R. Wilke, P. Chang, Correlation of diffusion coefficients in dilute solutions, AIChE J. 1 (2) (1955) 264–270.